Supplementary Information

Donor Modulation Brings All-In-One Phototheranostics for NIR-II Imaging-Guided Type-I Photodynamic/Photothermal Synergistic Cancer Therapy

*Yuxin Ren, Xinyi Zhang, Ling Li, Qiong Yuan, Benkai Bao, Meiqi Li, and Yanli Tang**

Key Laboratory of Analytical Chemistry for Life Science of Shaanxi Province, Key Laboratory of Applied Surface and Colloid Chemistry, Ministry of Education, School of Chemistry and Chemical Engineering, Shaanxi Normal University, Xi'an 710119, P. R. China

*Corresponding author. Email: yltang@snnu.edu.cn.

Content

1. Experimental Section

Materials and measurements.

All reagents used in organic synthesis experiments were purchased from Sinopharm Chemical Reagent Co. Ltd. (Beijing, China), Bide Pharmatech Co. Ltd. (Shanghai, China) or J&K Chemical Ltd. (Beijing, China), and directly used without further purification. DSPE-PEG_{2000} and DSPE-PEG_{2000}-cRGD were purchased from Ruixi Biological Technology Co. Ltd. (Xi'an, China). The 2', 7'-dichlorodihydrofluorescein diacetate (DCFH-DA), 9,10-Anthracenediyl-bis(methylene) dimalonic Acid (ABDA), Dihydroethidium (DHE) were purchased from Aladdin Industrial Corporation (Shanghai, China). Dihydrorhodamine 123 (DHR 123) was purchased from Macklin Biochemical Technology Co. Ltd. (Shanghai, China). 5,5-dimethyl-1-pyrroline N-oxide (DMPO) and 2,2,6,6-tetramethyl-4-piperidone hydrochloride (TEMP) were purchased from DOJINDO Laboratories (Japan). 3-(4, 5-dimethylthiazol-2-yl)-2, 5 diphennyltetrazolium bromide (MTT), Calcein Acetoxymethyl Ester (Calcein AM) and Propidium Iodide (PI) were purchased from Sigma-Aldrich (St. Louis, MO). 10× phosphate buffer solution (PBS) was purchased from Sangon Biotech Co. Ltd (Shanghai, China). Roswell Park Memorial Institute (RPMI) 1640 medium, Dulbecco's Modified Eagle Medium (DMEM), Fetal Bovine Serum (FBS), Penicillin-Streptomycin (100X) and 0.25% (1×) Trypsin were obtained from Gibco.

^{1}H NMR and ^{13}C NMR spectra were recorded on Bruker Avance 400 or 600 MHz spectrometers. The mass spectra were recorded on Bruker microflex MALDI-TOF or Bruker Autoflex speed MALDI-TOF. The UV-vis absorption spectra were taken on a Shimadzu UV-2600 spectrophotometer. The fluorescence emission spectra were recorded on a Horiba

Fluorolog-QM spectrophotometer. The EPR spectra were measured on Bruker E500 (Germany). The size distribution was measured on dynamic light scattering (DLS) (Malvern Zetasizer 3000HS). Cell numbers were quantitated using an Accuri C6 flow cytometer (Becton 110 Dickinson, Franklin Lakes, NJ). The absorbance for MTT analysis were performed on a microplate reader (SpectraMax M5). Fluorescence imaging experiments of cells were performed on an inverted fluorescence microscope (Olympus IX73). Confocal laser scanning microscopy images were recorded on Olympus FV1200. The fluorescence images in vitro and in vivo were collected on NIROPTICS series III 900/1700.

Synthesis of compound 1.[1]

An oven-dried Schlenk flask was filled with 4-aminoacetophenone (270 mg, 2.05 mmol), CuI (76 mg, 0.41 mmol), 4-iodoanisole (1.2 g, 5.13 mmol), KOH (840 mg, 15.00 mmol) and 1,10-Phenanthroline (83 mg, 0.51 mmol), evacuated and back-filled with nitrogen. Then toluene (20 mL) was added and the reaction was stirred at 100 ^{o}C for 24 h. After the reaction stopped, the mixed solution was extracted with dichloromethane and washed with saturated saline solution. The organic layer was evaporated under reduced pressure and purified by column chromatography with petroleum ether/ethyl acetate (v/v=5:1) to give a white solid (208 mg, 30% Yield). ^{1}H NMR (400 MHz, Chloroform-d), δ (ppm): 7.75 (d, J = 8.9 Hz, 2H), 7.11 (d, J = 8.9 Hz, 4H), 6.88 (d, J = 8.9 Hz, 4H), 6.81 (d, J = 8.9 Hz, 2H), 3.81 (s, 6H), 2.50 (s, 3H). ^{13}C NMR (151 MHz, Chloroform-d) δ 196.31, 157.05, 152.91, 139.24, 130.00, 128.25, 127.86, 116.84, 115.00, 55.50, 26.16. MALDI-TOF-MS: calculated for $C_{22}H_{21}NO_3^+$ $[M-H]^+$ 346.15, found 346.0.

Synthesis of compound 2.[2]

4-methoxy-N-(4-methoxyphenyl)-N-phenylaniline (2 g, 6.55 mmol) and $POCl_3$ (0.9 mL, 9.66 mmol) were dissolved with DMF (24 mL). The mixture was stirred and heated under reflux (90 °C) for 3 h. After the reaction stopped, the mixed solution was extracted with dichloromethane and washed with saturated saline solution. The organic layer was evaporated under reduced pressure and purified by column chromatography with dichloromethane/ petroleum ether (v/v=2:1) to give a green solid (2.182 g, 80% Yield). ^{1}H NMR (400 MHz, Chloroform-d), δ (ppm): 9.73 (s, 1H), 7.61 (d, *J* = 8.2 Hz, 2H), 7.12 (d, *J* = 8.1 Hz, 4H), 6.86 (dd, *J* = 15.6, 8.2 Hz, 6H), 3.79 (s, 6H). ^{13}C NMR (151 MHz, Chloroform-d) δ 190.12, 157.34, 154.05, 138.75, 131.39, 128.06, 127.74, 116.69, 115.09, 55.44. MALDI-TOF-MS: calculated for $C_{21}H_{19}NO_3^+$ $[M-2H]^+$ 331.14, found 331.6.

Synthesis of compound 3.

compound 1 (1.88 g, 5.25 mmol) and **compound 2** (1.75 g, 5.25 mmol) was dissolved in EtOH (15 mL), then NaOH solution (1.00 g in 2 mL H_2O) was dropped. After the reaction stopped, the mixed solution was extracted with dichloromethane and washed with saturated saline solution. The organic layer was evaporated under reduced pressure and purified by column chromatography with petroleum ether/ethyl acetate (v/v=20:1) to give an orange solid (2.54 g, 67% Yield). ^{1}H NMR (400 MHz, Chloroform-d), δ (ppm): 7.85 (d, *J* = 8.2 Hz, 2H), 7.75 (d, *J* = 15.4 Hz, 1H), 7.42 (d, *J* = 8.0 Hz, 2H), 7.35 (d, *J* = 15.4 Hz, 1H), 7.11 (t, *J* = 9.8 Hz, 8H), 6.87 (t, *J* = 7.6 Hz, 12H), 3.81 (s, 12H). ^{13}C NMR (151 MHz, Chloroform-d) δ 188.04, 156.96, 156.61, 152.56, 150.68, 143.36, 139.85, 139.40, 130.07, 129.64, 129.57,

127.79, 127.38, 126.60, 118.84, 118.39, 117.23, 114.96, 114.88, 55.51. MALDI-TOF-MS: calculated for $C_{43}H_{38}N_2O_5^+$ $[M]^+$ 662.28, found 662.7.

Synthesis of compound 4.

compound 3 (1.04 g, 1.58 mmol) and nitromethane (840 μL, 15.80 mmol) was dissolved in a mixture of ethyl alcohol (25 mL) and diethylamine (1.62 mL 15.80 mmol), The mixture was stirred and heated under reflux (115 °C) for overnight. The crude product was extracted with ethyl acetate. Na_2SO_4 was used to dry the combined organics. Solvent was cleaned up under reduced pressure. The final product was acquired by chromatography (petroleum ether/ethyl acetate: 20:1) to give a yellow solid (792 mg, 70%). ^{1}H NMR (600 MHz, Chloroform-d) δ 7.70 (d, *J* = 8.9 Hz, 2H), 7.10 (d, *J* = 8.9 Hz, 4H), 7.02 (t, *J* = 9.5 Hz, 6H), 6.88 (d, *J* = 8.9 Hz, 4H), 6.85 – 6.75 (m, 8H), 4.78 (dd, *J* = 12.4, 6.3 Hz, 1H), 4.62 (dd, *J* = 12.4, 8.3 Hz, 1H), 4.14 – 4.07 (m, 1H), 3.79 (d, *J* = 15.3 Hz, 12H), 3.31 (dd, *J* = 17.0, 6.1 Hz, 1H), 3.22 (dd, *J* = 17.0, 7.9 Hz, 1H). ^{13}C NMR (151 MHz, Chloroform-d) δ 195.04, 157.19, 155.90, 153.21, 148.19, 140.78, 139.00, 130.85, 129.81, 127.95, 127.93, 127.30, 126.66, 120.49, 116.69, 115.04, 114.70, 79.86, 55.49, 41.08, 39.03. MALDI-TOF-MS: calculated for $C_{44}H_{41}N_3O_7^+$ $[M\text{-}NO_2]^+$ 677.29, found 677.1.

Synthesis of compound 5.

compound 4 (235 mg 0.33 mmol) was dissolved in n-butanol (10 mL), then ammonium acetate (752 mg, 9.75 mmol) was dropped. the mixture was stirred under nitrogen at reflux for 24 h. After solvent was removed, the residue was filtered and washed with cool ethanol three times to give a black solid (110 mg, 30%). ^{1}H NMR (400 MHz, Chloroform-d),

δ (ppm): 8.22 (d, *J* = 8.3 Hz, 2H), 7.72 (dd, *J* = 5.6, 3.4 Hz, 1H), 7.60 (d, *J* = 8.6 Hz, 2H) 7.53 (dd, *J* = 5.7, 3.3 Hz, 1H), 7.12 (d, *J* = 8.6 Hz, 8H), 6.99 (d, *J* = 8.9 Hz, 10H), 6.93 (d, *J* = 7.5 Hz, 4H), 6.87 (d, *J* = 8.8 Hz, 8H), 6.84 – 6.73 (m, 12H), 5.30 (s, 2H), 3.79 (d, *J* = 22.1 Hz, 24H). ^{13}C NMR (151 MHz, Chloroform-d) δ 156.49, 155.85, 153.64, 150.01, 149.53, 148.20, 140.86, 140.05, 129.74, 127.88, 127.39, 127.17, 126.49, 124.01, 120.41, 119.72, 116.85, 115.01, 114.89, 114.71, 112.62, 55.51. MALDI-TOF-MS: calculated for $C_{88}H_{75}N_7O_8^+$ $[M]^+$ 1357.57, found 1357.4.

Synthesis of OTAB.

compound 5 (110 mg 0.08 mmol) was dissolved in a mixture of dry CH_2Cl_2 (10 mL), DIPEA (282 μL 1.62 mmol) and BF_3•OEt_2 (200 μL 1.62 mmol). the crude product was extracted with CH_2Cl_2. Na_2SO_4 was used to dry the combined organics. Solvent was cleaned up under reduced pressure. The final product was acquired by chromatography (CH_2Cl_2/ petroleum ether: 5:1) to give a blue solid (94 mg, 82%). ^{1}H NMR (400 MHz, Chloroform-d), δ (ppm): 7.94 (d, *J* = 8.9 Hz, 4H) 7.88 (d, *J* = 8.9 Hz, 4H) 7.13 (d, *J* = 8.9 Hz, 8H) 7.08 (d, *J* = 8.9 Hz, 8H) 6.88 (t, *J* = 8.9 Hz, 18H) 6.82 (d, *J* = 9.0 Hz, 8H) 3.80 (d, *J* = 9.6 Hz, 24H). ^{13}C NMR (151 MHz, Chloroform-d) δ 156.77, 156.29, 155.95, 150.44, 149.23, 145.27, 140.24, 139.58, 130.80, 129.96, 127.71, 127.00, 126.70, 125.03, 122.85, 120.31, 119.45, 118.01, 114.86, 114.78, 114.70, 55.50. ^{19}F NMR (376 MHz, Chloroform-d) δ (ppm): -131.27 – -131.64 (m, BF_2). MALDI-TOF-MS: calculated for $C_{88}H_{74}BF_2N_7O_8^+$ $[M]^+$ 1405.57, found 1405.3.

DFT calculation.

All the calculations of OTAB were based on density functional theory (DFT) with B3LYP/6-31G.[3] All these calculations were performed with Gaussian 16 program. THF was used as the solvent.

Preparation of nanoparticles.

Preparation of OTAB@cRGD NPs. THF solution (1 mL) containing DSPE-PEG_{2000}-cRGD (10 mg) and OTAB (1 mg) were added dropwise into an aqueous solution (10 mL), and the mixture was stirred for 12 h at ambient temperature to evaporate THF. The aqueous solution was centrifuged with a centrifugal-filter (MWCO = 3500 Da) at 5000 r for 15 min and filtered through a 0.22 μm filter for subsequent experiments.

Preparation of OTAB@cRGD-NR NPs: THF solution (1 mL) containing DSPE-PEG_{2000}-cRGD (10 mg), OTAB (1 mg) and Nile Red (0.5 mg) were added dropwise into an aqueous solution (10 mL), and the mixture was stirred for 12 h at ambient temperature to evaporate THF. The aqueous solution was centrifuged with a centrifugal-filter (MWCO = 3500 Da) at 5000 r for 15 min and filtered through a 0.22 μm filter for subsequent experiments.

OTAB NPs and **OTAB-NR NPs** were prepared in the same way as described above, except that DSPE-PEG_{2000}-cRGD was replaced by DSPE-PEG_{2000}.

Fluorescence quantum yield measurement.

The quantum yields of OTAB was calculated using ICG (QY = 13% in DMSO, Ex = 808 nm) as the reference fluorophore. The quantum yield was calculated as follows[4]:

$$\Phi_{unknown} = \Phi_{standard} \times \frac{S_{unknown}}{S_{standard}} \times \frac{\eta_{standard}^2}{\eta_{unknown}^2}$$

The UV-Vis absorbance values of OTAB or ICG at different concentrations were determined and the integrated fluorescence intensity was plotted from the absorbance values. Comparison of slopes yielded the quantum yield of OTAB@cRGD NPs.

Estimation for ROS production of cRGD@OTAB NPs.

The total ROS measurement by DCFH.[5] The ROS generation efficacy of OTAB@cRGD NPs was estimated by commonly-used ROS indicator DCFH-DA. DCFH-DA (0.97 mg) dissolved in DMSO (1 mM, 2000 μL) was mixed with NaOH (10 mM in dd water, 8 mL) followed by being reacted in dark place for 30 min to hydrolyze into DCFH. The activated DCFH-DA (DCFH, 40 μM) was added into the aqueous solution of OTAB@cRGD NPs (25 μg mL^{-1}), then the mixed solution was illuminated with 808 nm laser (808 nm, 1.0 W cm^{-2}) for various time interval. The fluorescence spectra of DCF (λ_{ex} = 488 nm, λ_{em} = 525 nm) induced by and OTAB@cRGD NPs-sensitized ROS was recorded.

$O_2^{\cdot-}$ measurement by DHR123.[6] DHR 123 (5 μM) and OTAB@cRGD NPs (25 μg mL^{-1}) in PBS solution were mixed and then exposed to laser irradiation (808 nm, 1.0 W cm^{-2}). The fluorescence peak at 530 nm was recorded after various irradiation times.

$O_2^{\cdot-}$ measurement by DHE.[7] DHE (40 μM) containing ctDNA (0.5 mg mL^{-1}) and OTAB@cRGD NPs (25 μg mL^{-1}) in PBS solution were mixed and then exposed to laser irradiation (808 nm, 1.0 W cm^{-2}). The fluorescence peak at 530 nm was recorded after various irradiation times.

$^1O_2$ measurement by ABDA.[8] ABDA (40 μM) and OTAB@cRGD NPs (25 μg mL^{-1}) in PBS solution were mixed and then exposed to laser irradiation (808 nm, 1.0 W cm^{-2}). The absorption peak at 378 nm was recorded after various irradiation times.

ESR measurement.

$^1O_2$ measuremen by ESR measurement. TEMP (0.06 M) was added into 100 μL of OTAB@cRGD NPs (25 μg mL^{-1}) in H_2O. The mixture was exposed to 808 nm laser (1.0 W cm^{-2}) for 5 min or left in the dark. Then $^1O_2$ was indicated by the ESR signal.

$O_2^{\cdot-}$ measurement by ESR measurement. A 10 μL amount of DMPO was added into 90 μL of OTAB@cRGD NPs (25 μg mL^{-1}) in Methanol. The mixture was exposed to 808 nm laser (1.0 W cm^{-2}) for 5 min or left in the dark. Then $O_2^{\cdot-}$ was indicated by the ESR signal.

·OH measurement by ESR measurement. A 10 μL amount of DMPO was added into 90 μL of OTAB@cRGD NPs (25 μg mL^{-1}) in H_2O. The mixture was exposed to 808 nm laser (1.0 W cm^{-2}) for 5 min or left in the dark. Then ·OH was indicated by the ESR signal.

Photothermal performance.

The Photothermal conversion efficiency was calculated by following equation: [9]

$$\eta = \frac{hS\Delta T_{max} - Q_{Dis}}{I(1 - 10^{-A_{808}})} \quad (1)$$

$$hS = \frac{m_s C_s}{\tau} \quad (2)$$

$$t = -\tau \ln(\theta) \quad (3)$$

$$\theta = \frac{\Delta T}{\Delta T_{max}} \quad (4)$$

η denotes the photothermal conversion efficiency, h represents the heat transfer coefficient, S means the surface area of the container. ΔT_{max} is the maximum temperature change of the samples under laser irradiation, Q_{dis} means the heat dissipated from the solution and container, I means the laser power, A_{808} is the absorbance of OTAB@cRGD NPs (50 μg mL^{-1}) at 808 nm. In equation (2), m_s is the mass of the solution and c_s is the heat capacity of the solution. τ can be obtained from the linear fitting of time versus -ln(θ) by equation (3). As shown in Fig 3e, τ was calculated as 234.51 s. In equation 2, The hS was calculated as 0.034 W/℃. Q_{dis} was 0.07014 W, respectively. ΔT_{max} was 20.8 ℃ according to experimental results. Thus, the photothermal conversion efficiency was calculated as 29.7% by equation (1).

Cell culture.

4T1 cells (mouse breast cancer cell line) were cultured in RPMI-1640 medium containing 10% FBS and 1% penicillin-streptomycin at 37 ℃ with 5% CO_2 in an incubator. MDA-MB-231 cells (human breast cancer cell line) and HUVEC (Human umbilical vein endothelial cell line) were cultured in DMEM containing 10% FBS and 1% penicillin-streptomycin at 37 ℃ with 5% CO_2 in an incubator.

Cytotoxicity by MTT assay.

The dark cytotoxicity of OTAB NPs and OTAB@cRGD NPs against HUVEC, 4T1 and MDA-MB-231 cells was evaluated by MTT assay according to the reported procedure.[10]

The phototoxicity of OTAB NPs and OTAB@cRGD NPs against 4T1 and MDA-MB-231 cells was also evaluated by the MTT assay. The cells were incubated with medium containing different concentrations of OTAB NPs and OTAB@cRGD NPs for 12 h and irradiated with

808 nm laser (1.0 W cm^{-2}) for 5 min. Then cells were incubated for another 24 h, and the cell viability was measured.

Live/dead co-staining assay.

1 × 10^5 4T1 cells were seeded in a 96-well plate overnight and divided into six groups (PBS, PBS + L, OTAB NPs, OTAB NPs + L, OTAB@cRGD NPs, and OTAB@cRGD NPs + L). For the NPs groups, cells were treated with the OTAB NPs and OTAB@cRGD NPs at a concentration of 25 μg mL^{-1} for 12 h, and washed with PBS three times. For the control groups, cells were cultured only with pure cell medium. After laser light irradiation (808 nm, 1.0 W cm^{-2}), all cells were coincubated with Calcein AM (4 μM) and PI (9 μM) for 30 min, washed with PBS three times and the fluorescence microscope images were obtained. The excitation wavelength was 488 nm for Calcein AM and 561 nm for PI.

Cellular uptake efficiency by NIR-II fluorescence imaging.[11]

4T1 cells were seeded in 6-well plates at a density of 5 × 10^4 cells and cultured them for 24 h. Then, the incubate medium was replaced with medium containing OTAB NPs or OTAB@cRGD NPs (25 μg mL^{-1}). After incubating for 0 h, 1 h, 3 h, 6 h and 10 h, the cells were digested with trypsin (EDTA) and centrifuged at 1000 rpm for 4 min. The cells were then washed three times with sterile PBS (10 mM, pH 7.4) buffer to remove the remaining culture medium, and they were reseeded in 96-well plates in PBS (100 μL). The 96-well plates were irradiated with the NIR-II fluorescence imaging system (808 nm laser, 0.3 W cm^{-2}, 1000 nm long-pass filter) to measure the NIR-II signal and analyze the targeting efficiency of OTAB@cRGD NPs NPs to breast cancer cells.

Intracellular uptake of OTAB-NR NPs and OTAB@cRGD-NR NPs.

MDA-MB-231 cells were seeded in a confocal culture dish (Nest) at a density of 105 per well for 18 h. Then, the incubate medium was replaced with 1 mL medium containing OTAB-NR NPs or OTAB@cRGD-NR NPs (25 μg mL^{-1}). After incubation for different times (0 h, 1 h, 3 h, 6 h), the old medium was removed and washed three times with PBS, and 1 mL fresh phenol red-free DMEM medium was added for confocal laser scanning microscopy.

ROS generation in cells.

MDA-MB-231 cells were seeded in a confocal culture dish at a density of 105 per well. Then OTAB@cRGD NPs (25 μg mL^{-1}) was add and cultured for 12 h under normoxic or hypoxic conditions. Subsequently, DCFH-DA (25 μM) was added. After incubating for 30 min, the cells were washed 3 times with PBS and then irradiated by laser (808 nm, 1.0 W cm^{-2}) for 5 min. The excitation wavelength for laser confocal imaging is 488 nm, and the emission wavelength range is 500–600 nm.

Ethical statement and animals model.

All animal procedures were performed in accordance with the Guidelines for Care and Use of Laboratory Animals of Shaanxi Normal University and approved by the Animal Ethics Committee of Shaanxi Normal University (20230207-1). BALB/c mice (female, 4-5 week, 15−20 g) were purchased from the Experimental Animal Center of Shaanxi Normal University. The right posterior region of BALB/c mice was injected with 1×10^6 4T1 cells *via* subcutaneous injection to obtain a 4T1 tumor-bearing mice model.

NIR-II fluorescence imaging.

4T1 tumor-bearing mice were anesthetized with isoflurane mixed with air, and intravenously injected with OTAB NPs and OTAB@cRGD NPs (200 μg mL^{-1}, 200 μL) and the fluorescence pictures were captured at different time intervals (0, 3, 6, 9, 12, 24, and 48 h). After 48 h, the mice were sacrificed and the fluorescence intensity of the tumor, heart, liver, lung, kidney and spleen were quantified.

***In vivo* phototherapy, photothermal imaging.**

When the tumor volume reached about 100 mm^3, the mice were randomly divided into 6 groups (n = 4). For the control groups (PBS and "PBS + L"), PBS (200 μL) was injected. For the OTAB NPs and "OTAB NPs + L" groups, the mice were injected with the OTAB NPs (200 μg mL^{-1}, 200 μL) in PBS solution, whilst for the OTAB@cRGD NPs and "OTAB@cRGD NPs + L" groups, the mice were injected with the cRGD@OTAB NPs (200 μg mL^{-1}, 200 μL) in PBS solution. 12 h after administration, the tumors of the "PBS + L" 、 "OTAB NPs + L" and "OTAB@cRGD NPs + L" groups were irradiated for 5 min with laser light (808 nm, 0.8 W cm^{-2}), the mice in the PBS group, OTAB NPs group, OTAB@cRGD NPs group were not irradiated. Tumor volume and body weight of the mice were measured every 2 days continuously for 16 days. The tumor size was calculated as follows: volume = (tumor length) × $(\text{tumor width})^2/2$. After the treatment, one mouse from each group was sacrificed for H&E and staining of the tumors. In addition, major organs (heart, liver, lung, kidney, and spleen) were isolated and fixed in 4% formaldehyde solution, followed by histology analysis. The images of the tissue sections were recorded on a microscope. For

photothermal imaging, the mice were injected with the OTAB NPs, OTAB@cRGD NPs (200 μg mL^{-1}, 200 μL) and PBS (200 μL). The tumors were irradiated with laser light (808 nm, 0.8 W cm^{-2}), the tumor temperature was captured by an IR camera.

Statistical analysis.

Unless otherwise stated, experimental conditions were performed in duplicate in at least three independent experiments. The Student's t-test was used for significance analysis and comparison of two samples. Data was expressed as the means ± SD. *P < 0.05, **P < 0.01, and ***P < 0.001.

2. Supplementary Figures

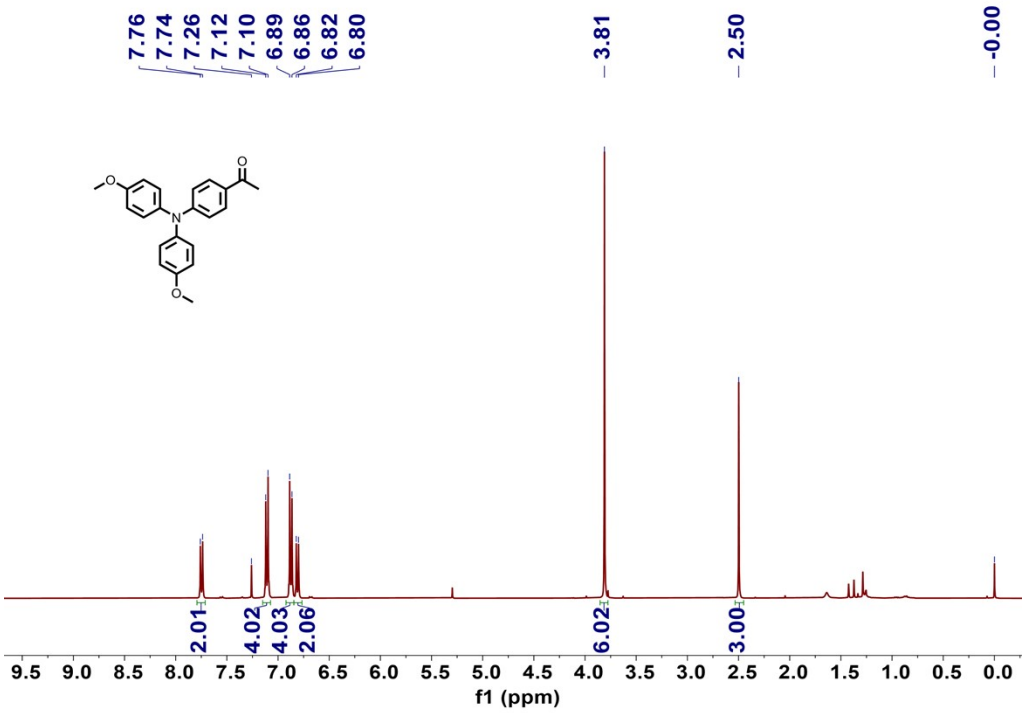

Fig. S1 ^{1}H NMR spectrum of compound 1 in $CDCl_3$.

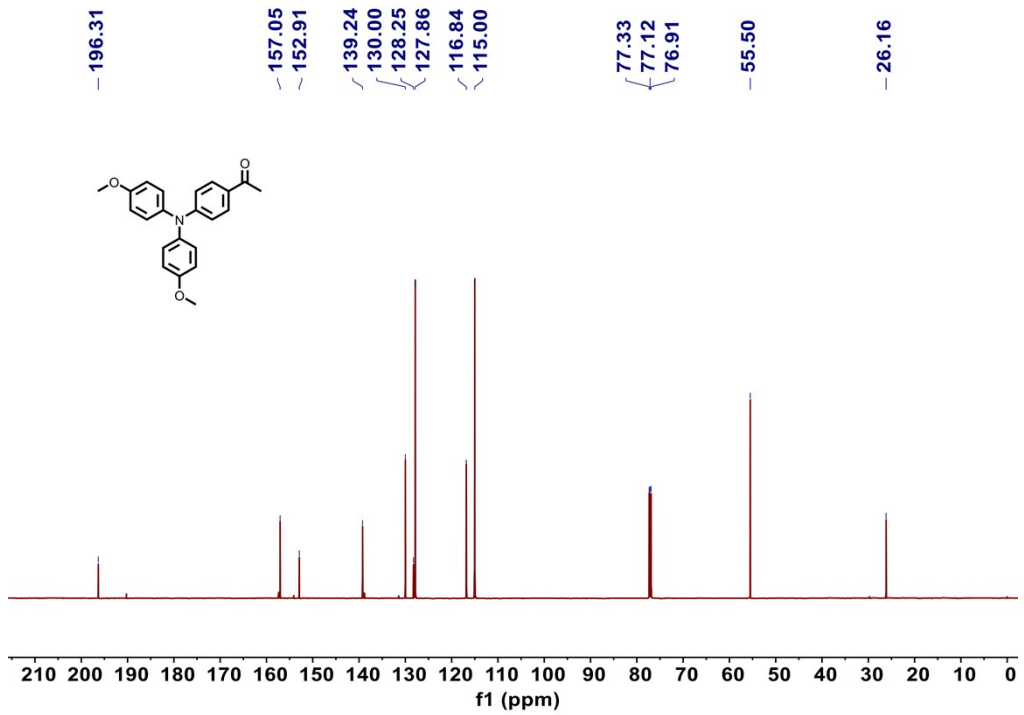

Fig. S2 ^{13}C NMR spectrum of compound 1 in $CDCl_3$.

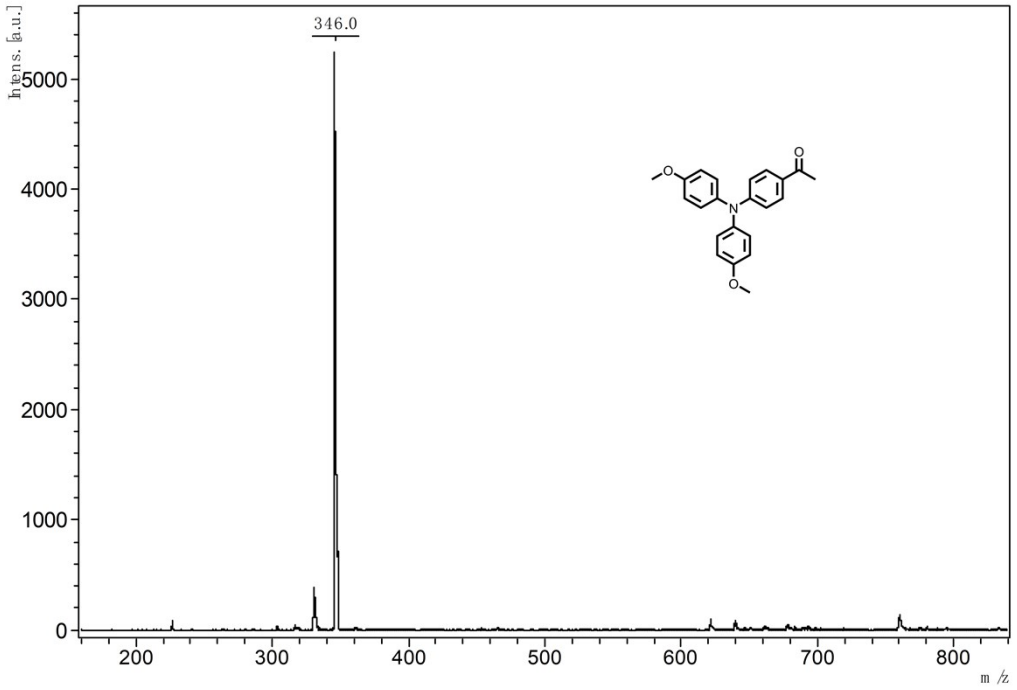

Fig. S3 MALDI-TOF-MS spectrum of compound 1.

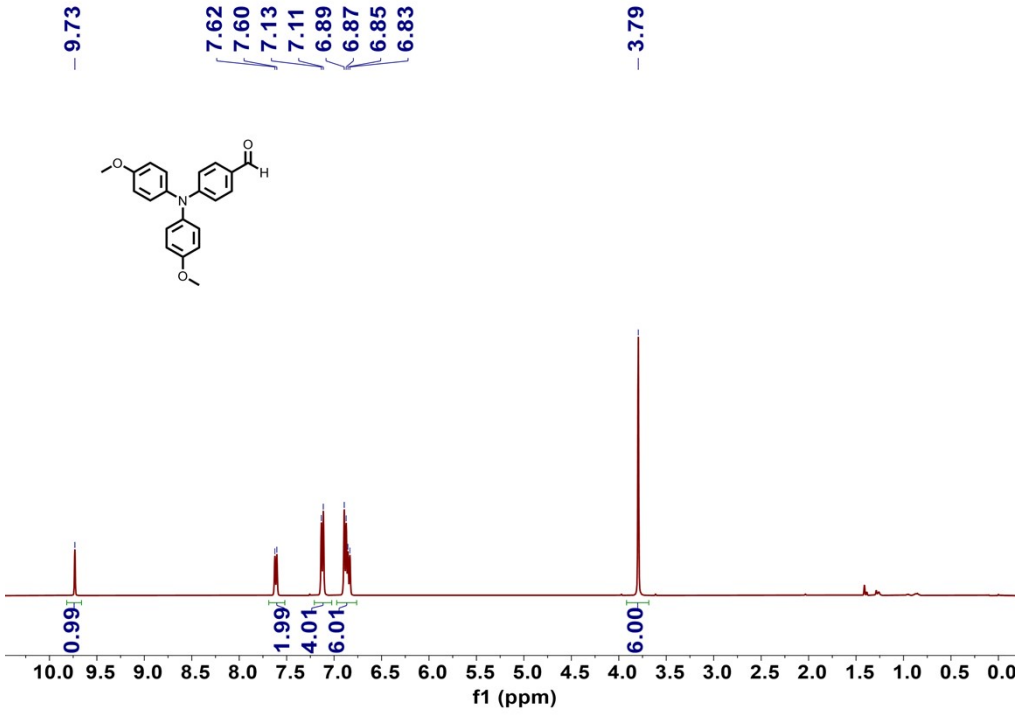

Fig. S4 ^{1}H NMR spectrum of compound 2 in $CDCl_3$.

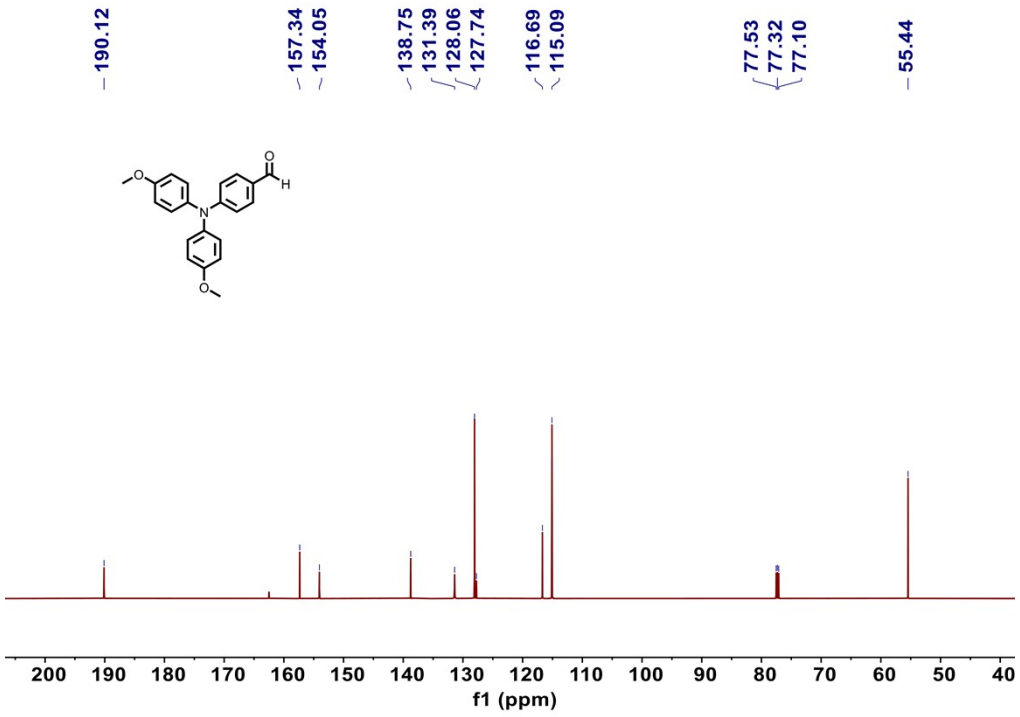

Fig. S5 ^{13}C NMR spectrum of compound 2 in $CDCl_3$.

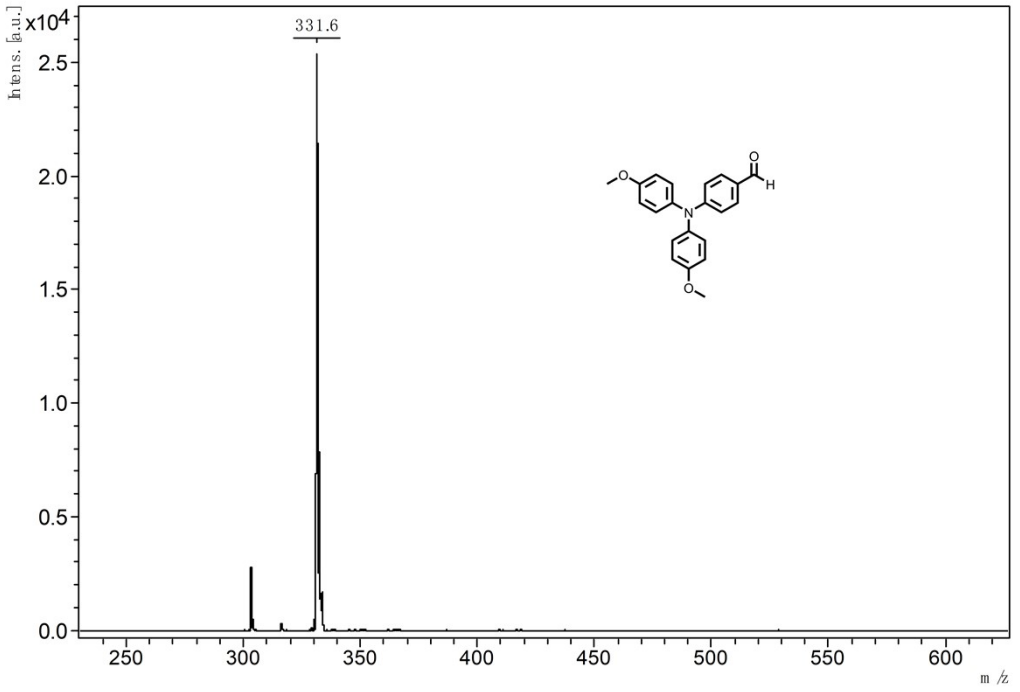

Fig. S6 MALDI-TOF-MS spectrum of compound 2.

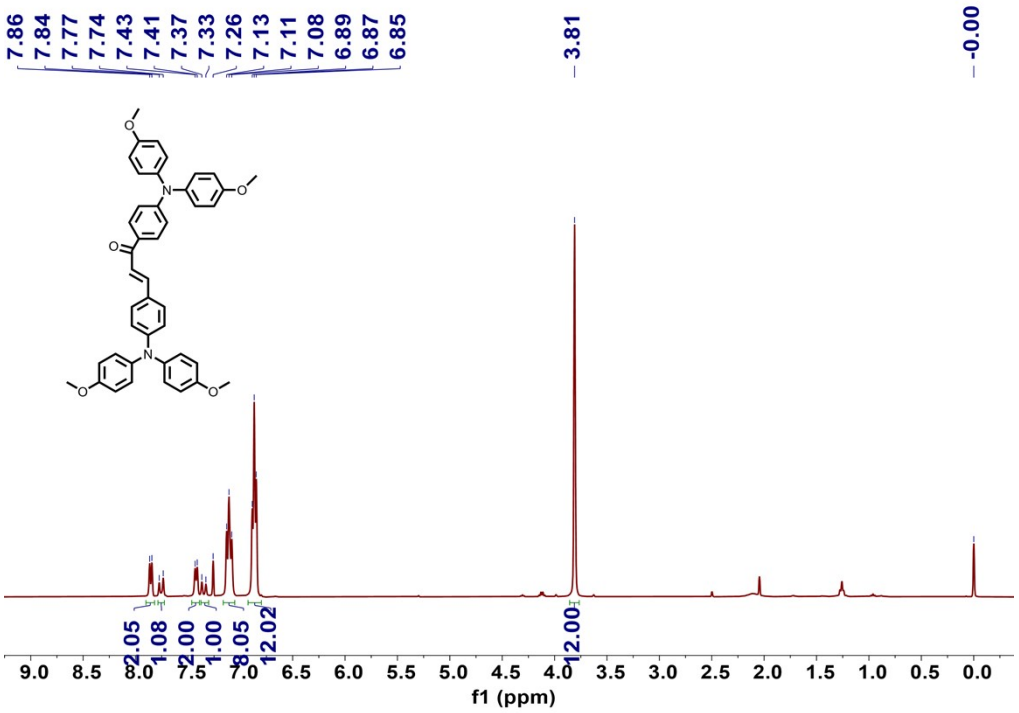

Fig. S7 ^{1}H NMR spectrum of compound 3 in $CDCl_3$.

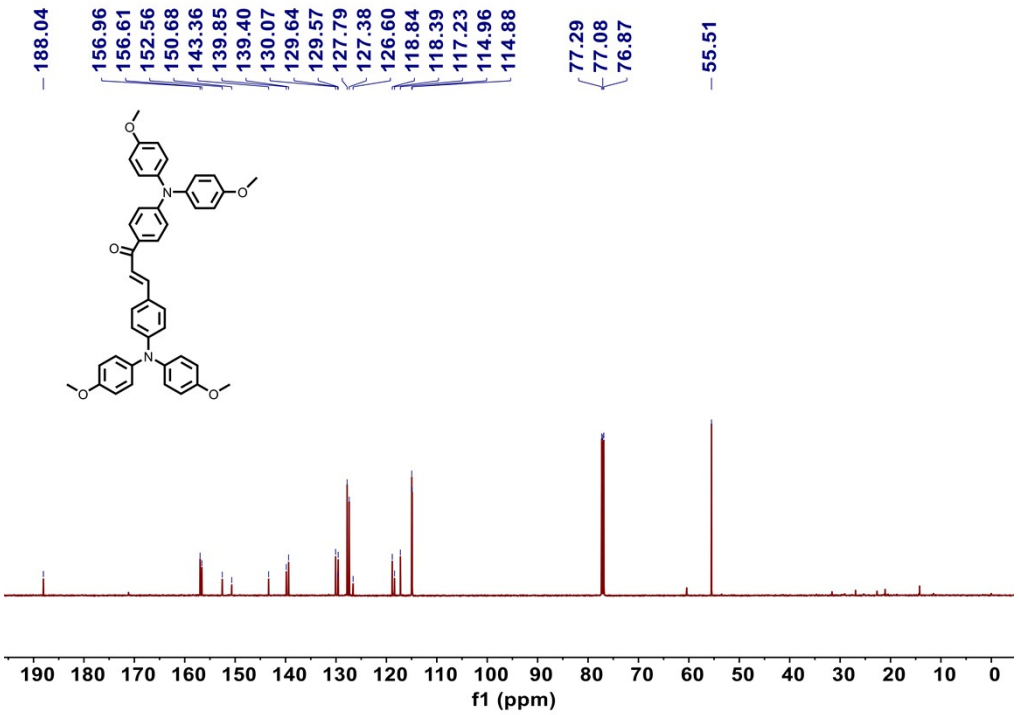

Fig. S8 ^{13}C NMR spectrum of compound 3 in $CDCl_3$.

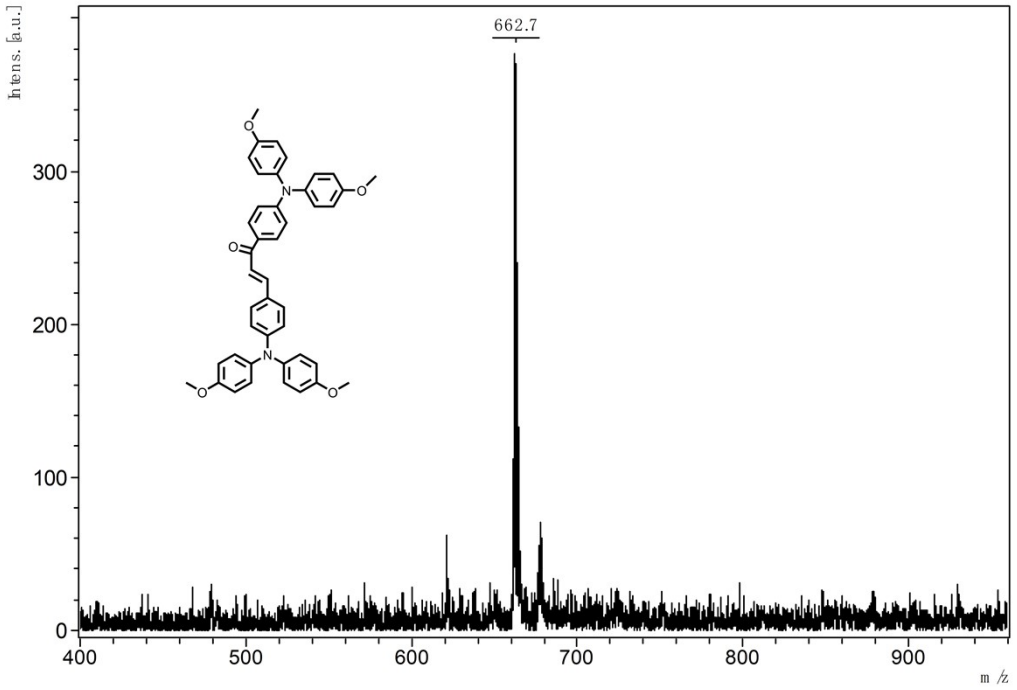

Fig. S9 MALDI-TOF-MS spectrum of compound 3.

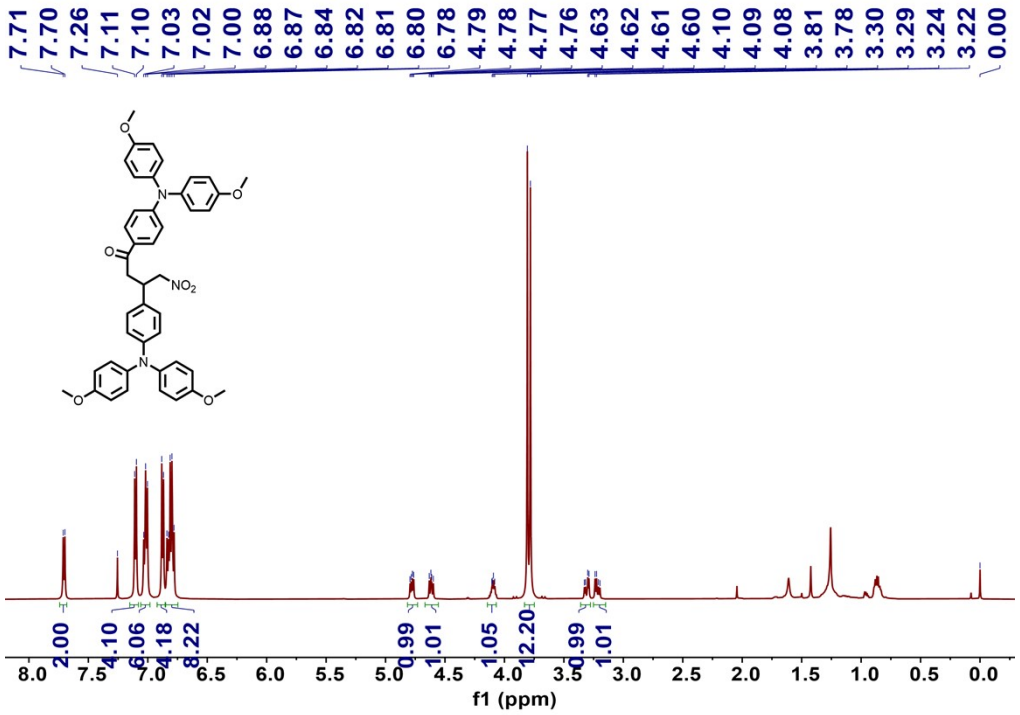

Fig. S10 ^{1}H NMR spectrum of compound 4 in $CDCl_3$.

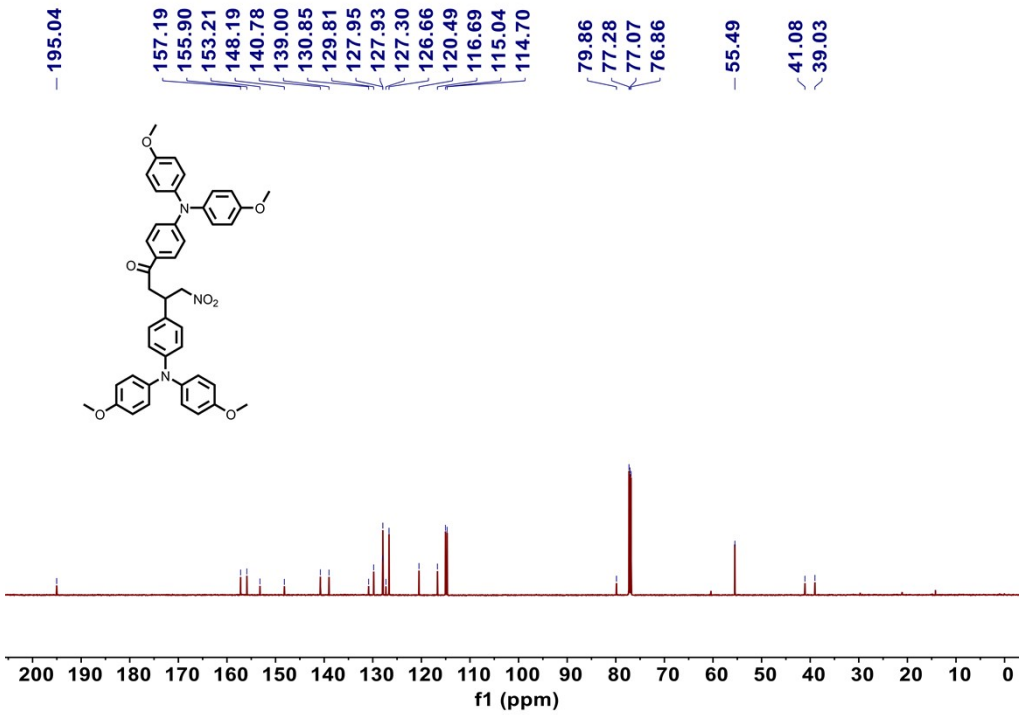

Fig. S11 ^{13}C NMR spectrum of compound 4 in $CDCl_3$.

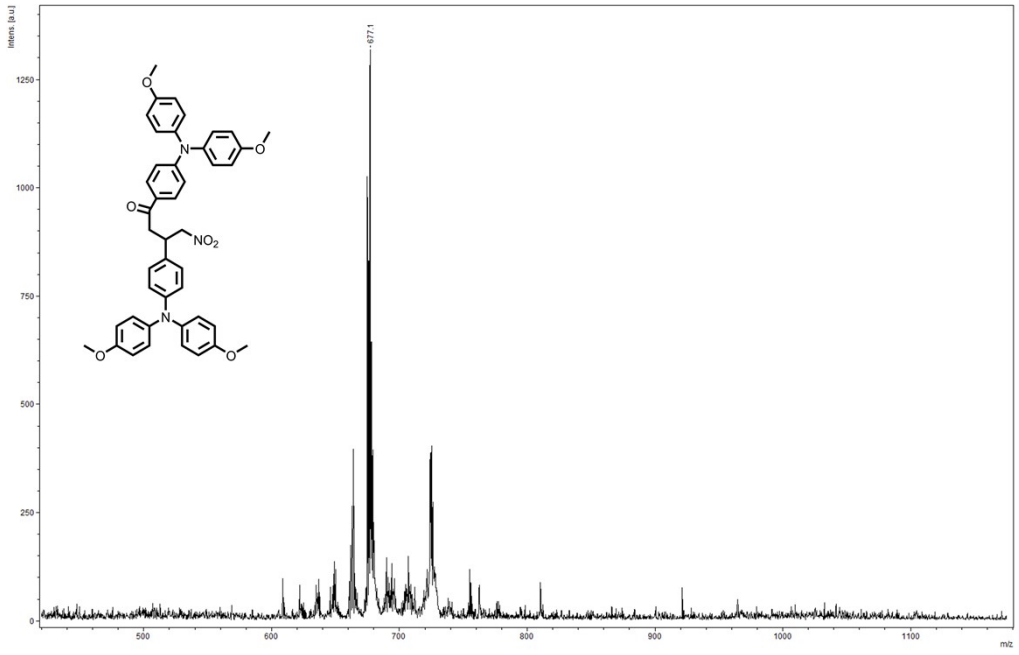

Fig. S12 MALDI-TOF-MS spectrum of compound 4.

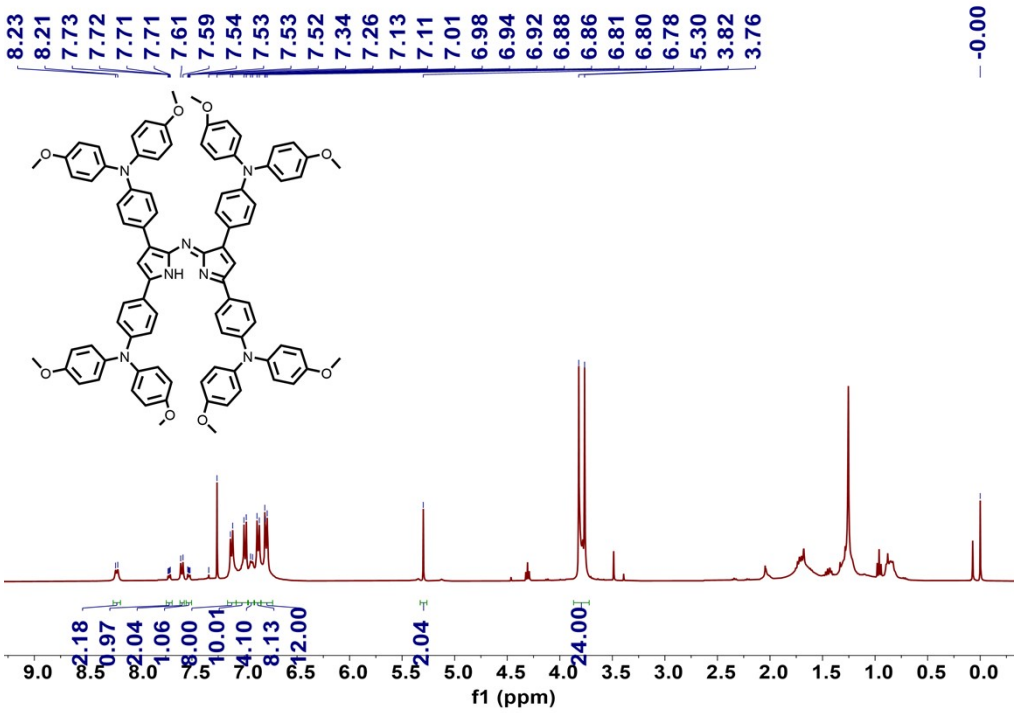

Fig. S13 ^{1}H NMR spectrum of compound 5 in $CDCl_3$.

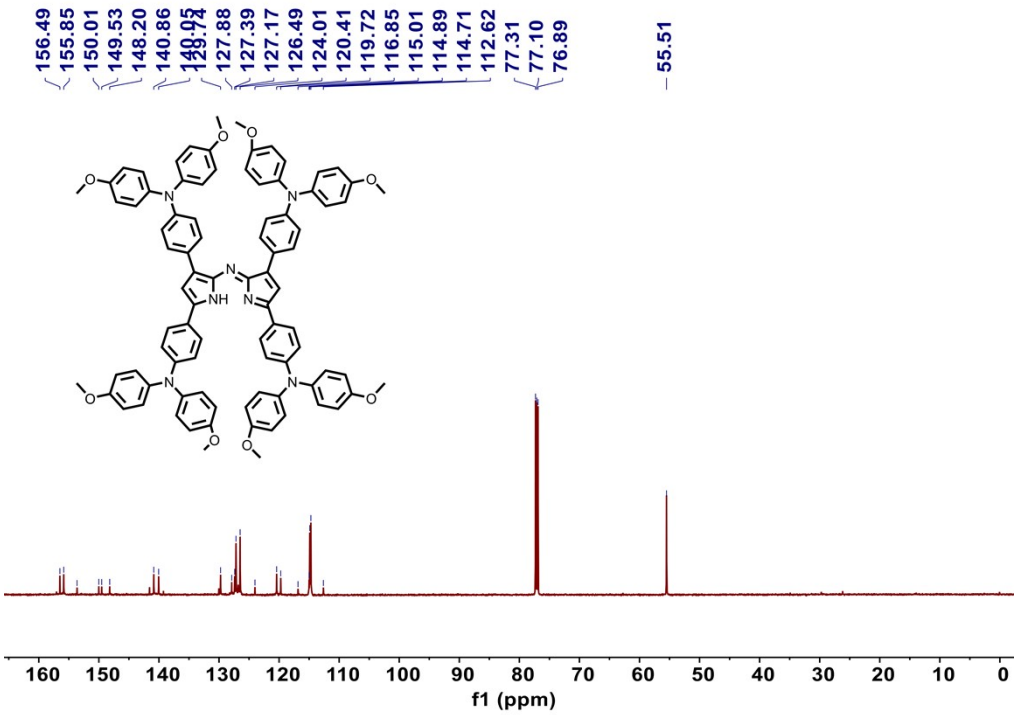

Fig. S14 ^{13}C NMR spectrum of compound 5 in $CDCl_3$.

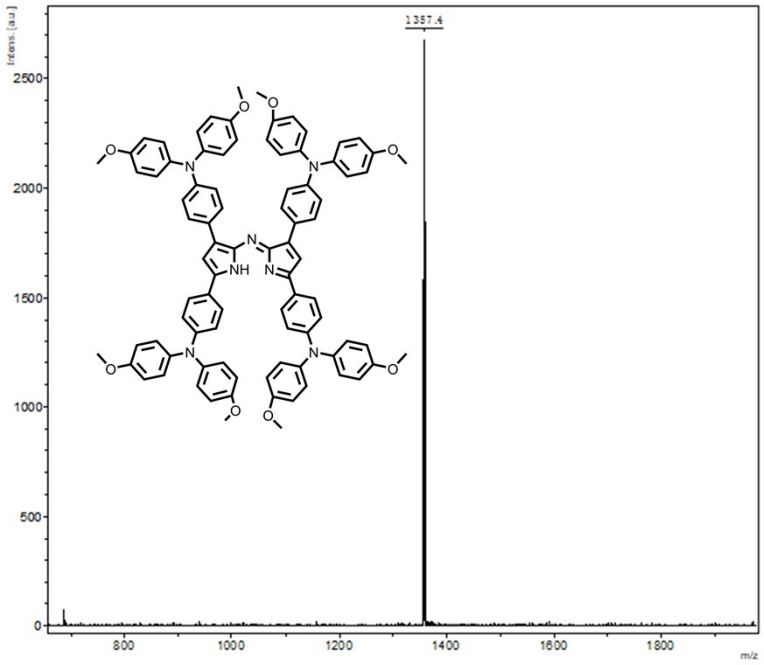

Fig. S15 MALDI-TOF-MS spectrum of compound 5.

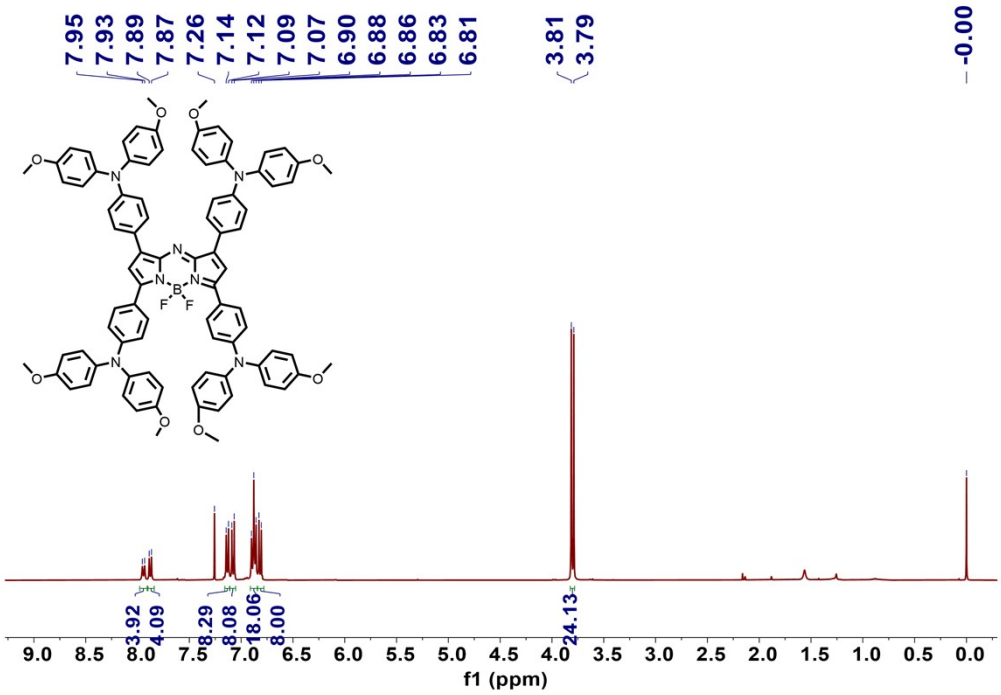

Fig. S16 ^{1}H NMR spectrum of OTAB in $CDCl_3$.

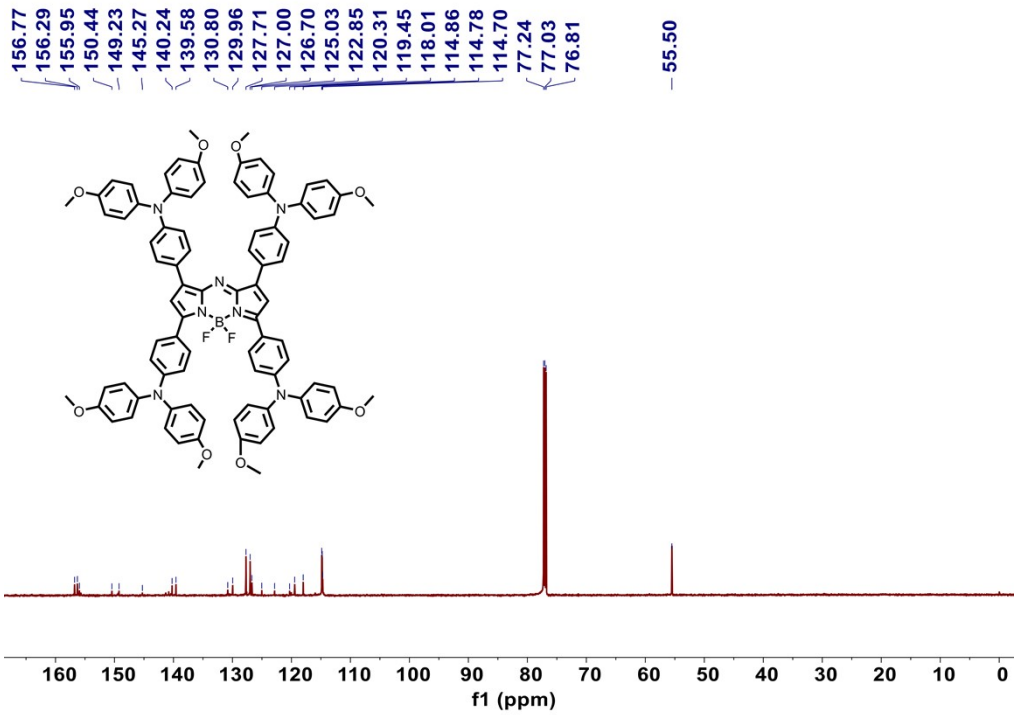

Fig. S17 ^{13}C NMR spectrum of OTAB in $CDCl_3$.

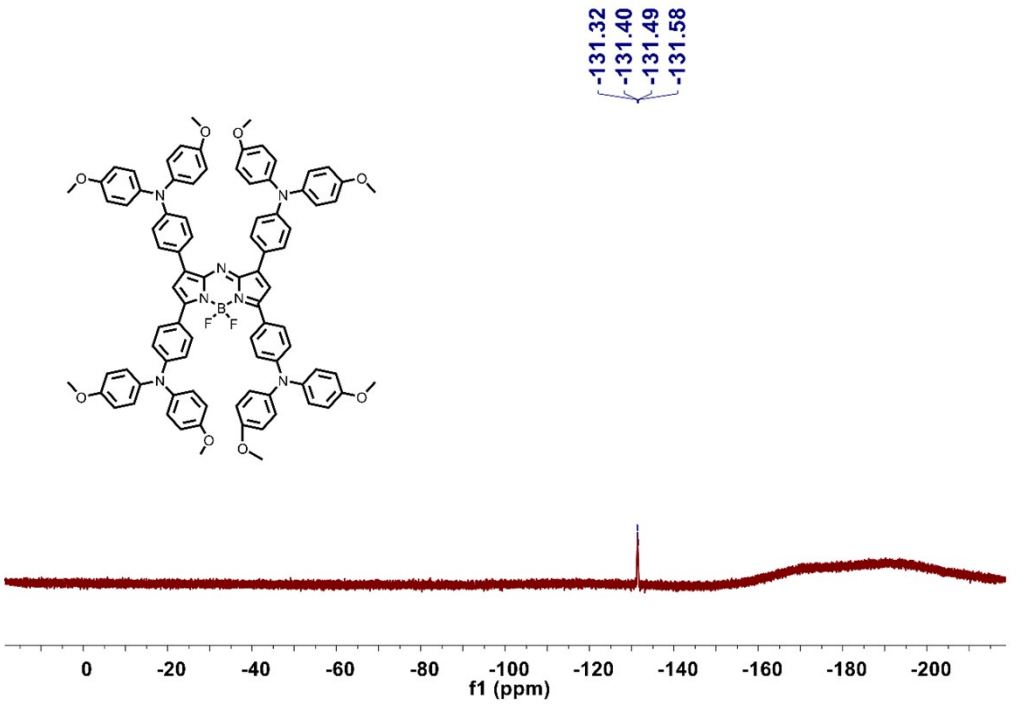

Fig. S18 ^{19}F NMR spectrum of OTAB in $CDCl_3$.

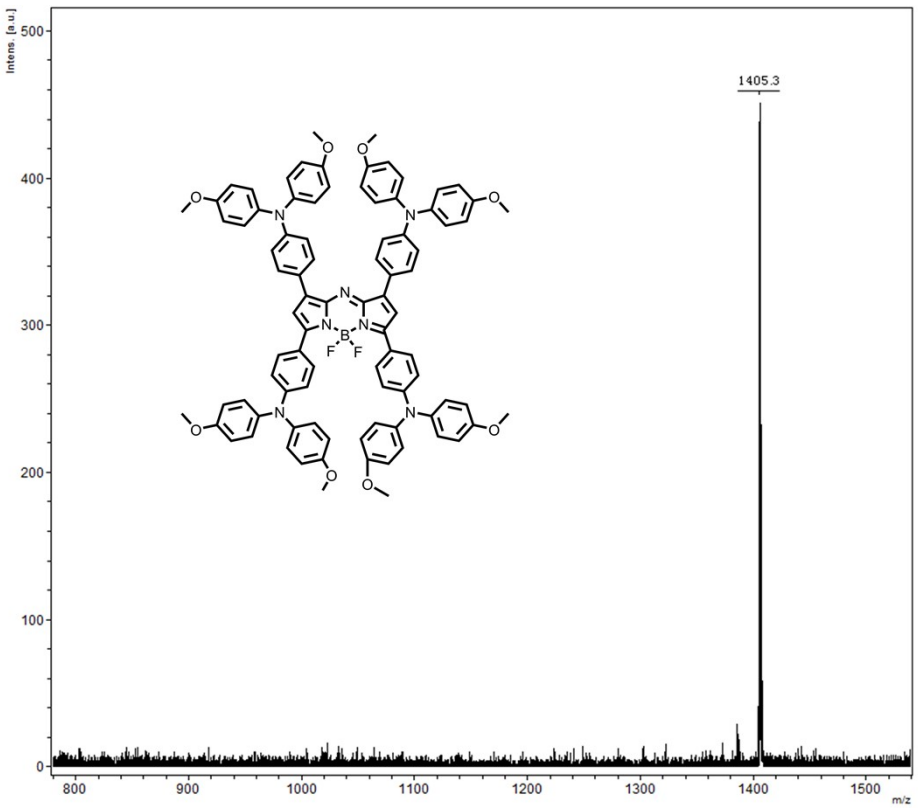

Fig. S19 MALDI-TOF-MS spectrum of OTAB.

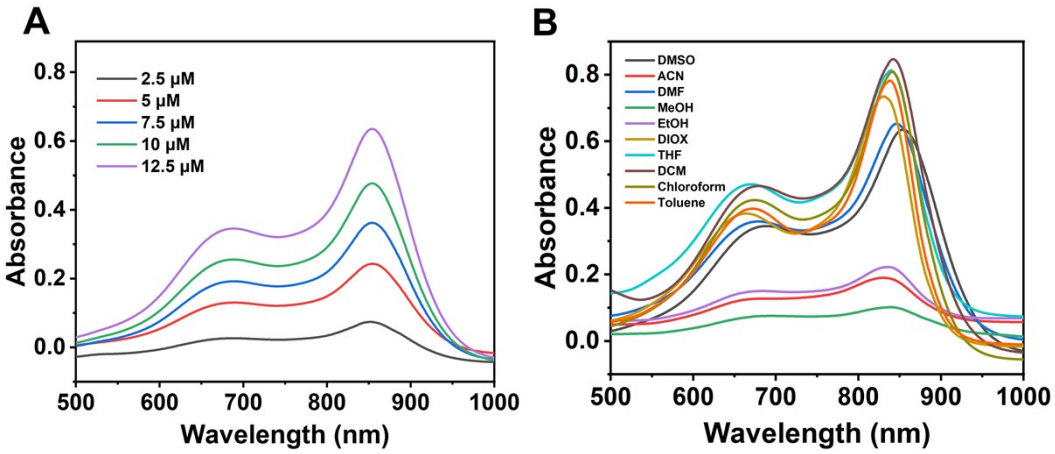

Fig. S20 Absorption spectra of (A) OTAB in various concentrations, (B) OTAB (12.5 μM) in various organic solvents. (DMSO: Dimethyl sulfoxide, ACN: Acetonitrile, DMF: N,N-Dimethylformamide, MeOH: Methanol, EtOH: Ethanol, DIOX: 1,4-Dioxane, THF: Tetrahydrofuran, DCM: Dichloromethane, Chloroform: Trichloromethane, Toluene: Methylbenzene)

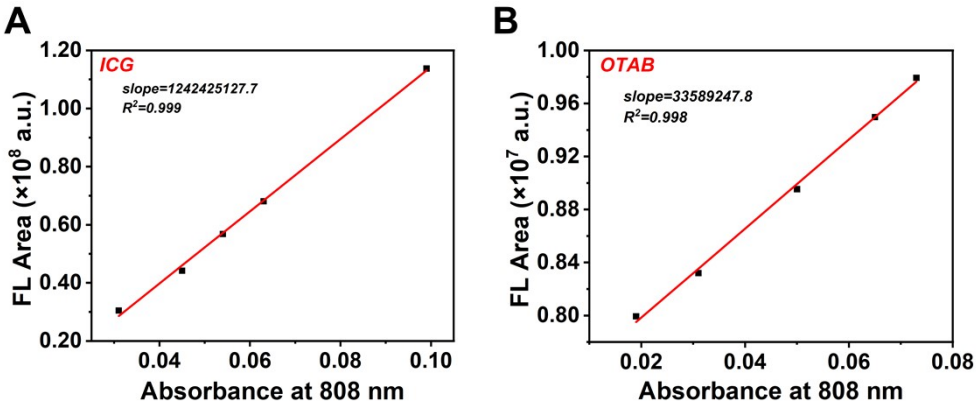

Fig. S21 Fluorescence quantum yield measurement of OTAB in DMSO. The integrated fluorescence intensity of (A) ICG and (B) OTAB in DMSO plotted as a function of absorbance at 808 nm.

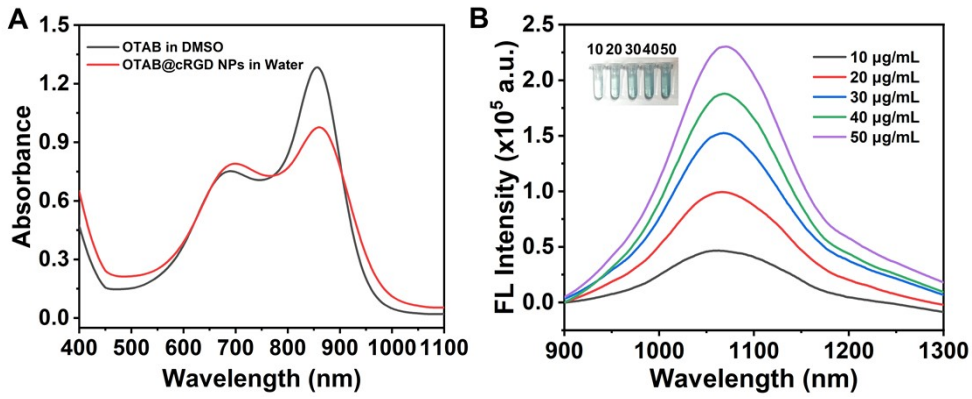

Fig. S22 (A) Absorption spectra of OTAB and aqueous OTAB@cRGD NPs. (B) Emission spectra of OTAB@cRGD NPs in various concentrations with corresponding photographs (inset).

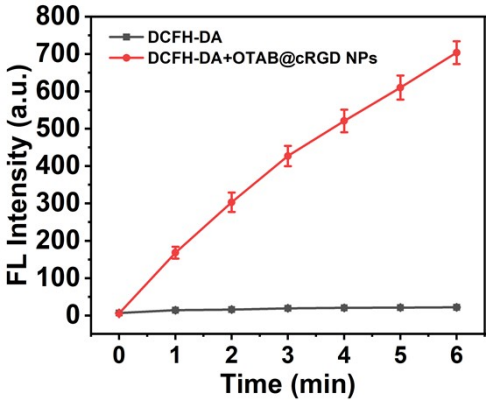

Fig. S23 Fluorescence intensity of DCF at 525 nm in the presence of OTAB@cRGD NPs under illumination (808 nm, 1.0 W cm^{-2}). [DCFH] = 40 μM, [OTAB@cRGD NPs] =25 μg mL^{-1}.

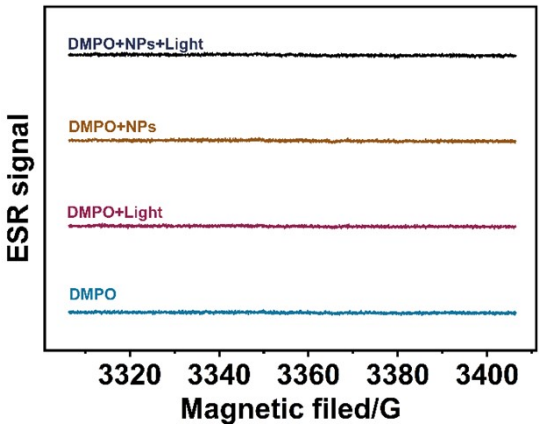

Fig. S24 ESR spectra to detect ·OH generated by OTAB@cRGD NPs (25 μg/mL) under illumination (808 nm, 1.0 W cm^{-2}), using DMPO as a spin trap agent.

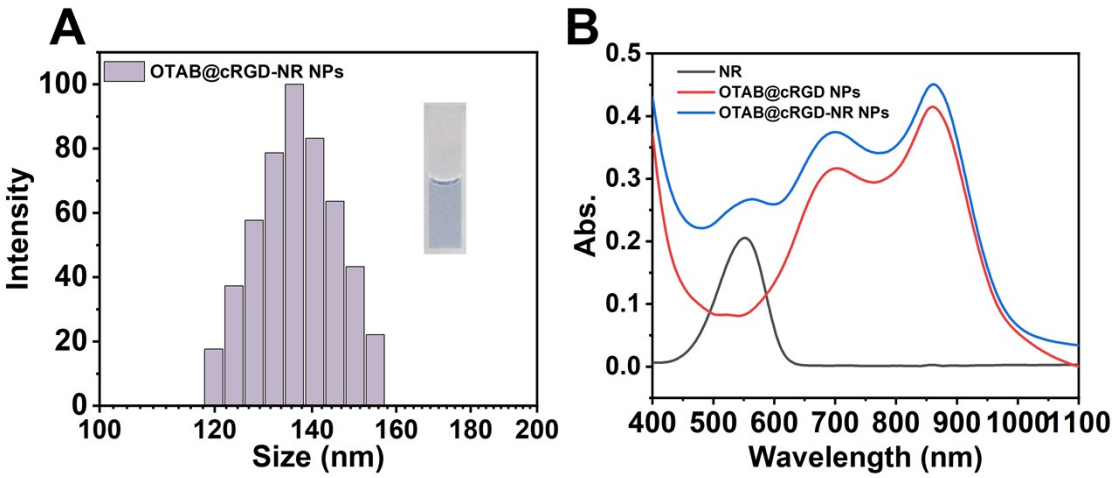

Fig. S25 (A) DLS data of OTAB@cRGD-NR NPs with corresponding photographs (inset). (B) Absorption spectra of NR, OTAB@cRGD NPs and OTAB@cRGD-NR NPs.

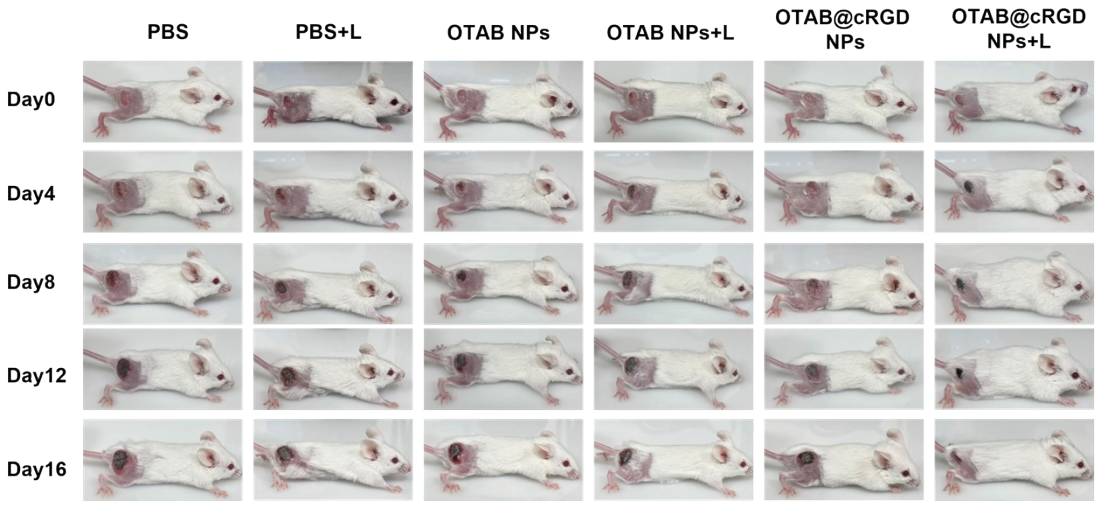

Fig. S26 Photographs of 4T1 tumor-bearing mice at Day 0, Day 4, Day 8, Day 12, and Day

16 of different groups.

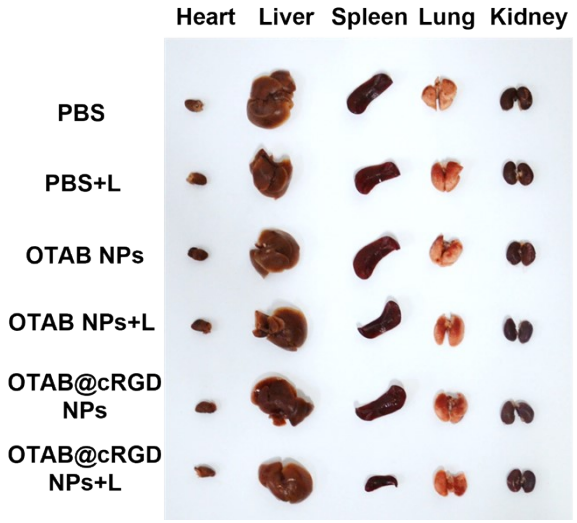

Fig. S27. Representative photographs of the main organs extracted from the mice in the various groups at the end of the treatments.

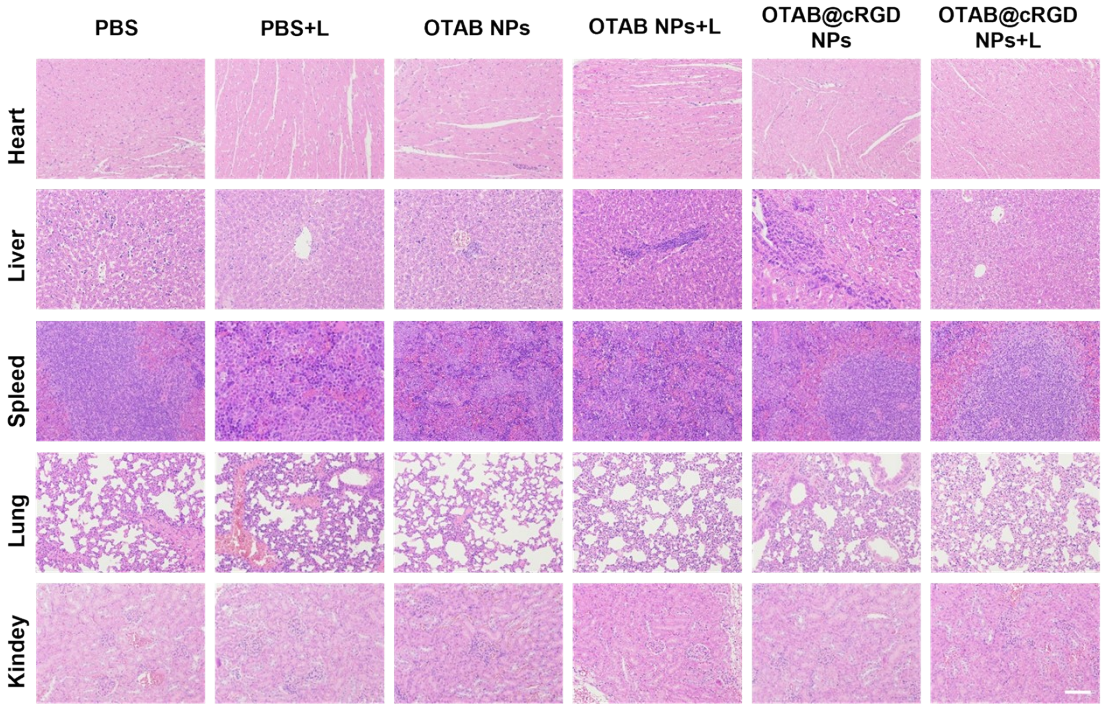

Fig. S28. H&E staining images of five major organs (heart, liver, spleen, lung, and kidney) in different treatments after the therapy for 4T1 tumor-bearing mice on day 16. Scale bar = 100 μm.

Table S1. Comparison of photophysical properties and imaging & therapeutic modalities of NIR-II aza-BODIPY dyes.

photosensitizers	$\lambda_{abs/em}$ (nm)	nanoparticles	$\lambda_{abs/em}$ (nm)	Imaging & therapeutic modalities	Ref.
NJ1060	910/1060	NJ1060 NPs	858/1062	NIR-II FLI	12
NIR998	859/998	NIR998 NPs	≈859/-	PTT	13
FBP 912	825/912	-	-	NIR-II FLI	14
Dye 2	843/920	J-NPs	946/1053	NIR-II FLI+PTT	15
CB1	860/1045	CB1 NPs	837/1015	NIR-II FLI+PTT	16
ABFe	810/-	ABFe NPs	725/-	NIR-II PAI+PTT	17
PTPE3	766/932	PTPE3 NPs	775/830-1400	NIR-II FLI+PDT	18
SW8	1030/1230	SW8@NPs	980/1000-1300	NIR-II FLI+PTT	19
BDP-TPE	792/880	P-TPE	812/1018	NIR-II FLI+PTT	20
OTAB	858/1050	OTAB@cRGD NPs	860/1069	NIR-II FLI +Type-I PDT+ PTT	This Work

3. References

(1) R. da Costa.; F. Farias.; L. Maqueira.; C. Castanho Neto.; L. Carneiro.; J. Almeida.; C. Buarque.; R. Aucélio.; J. Limberger, *J. Braz. Chem. Soc.,* 2019, **30**, 81.

(2) S. Chen.; P. Liu.; Y. Hua.; Y. Li.; L. Kloo.; X. Wang.; B. Ong.; W.-K. Wong.; X. Zhu, *ACS Appl. Mater. Interfaces,* 2017, **9**, 13231.

(3) W. Huang.; H. Yang.; Z. Hu.; Y. Fan.; X. Guan.; W. Feng.; Z. Liu.; Y. Sun, *Adv. Healthcare Mater.,* 2021, **10**, 2101003.

(4) Y. Yuan.; Z. Feng.; S. Li.; Z. Huang.; Y. Wan.; C. Cao.; S. Lin.; L. Wu.; J. Zhou.; L. S. Liao.; J. Qian.; C. S. Lee, *Adv. Mater.,* 2022, **34**, 2201263.

(5) B. Bao.; Q. Yuan.; Q. Feng.; L. Li.; M. Li and Y. Tang, *CCS Chemistry,* 2024, **6**, 693.

(6) P. Xiao.; Z. Shen.; D. Wang.; Y. Pan.; Y. Li.; J. Gong.; L. Wang.; D. Wang and B. Z. Tang, *Adv. Sci.,* 2021, **9**, 2104079.

(7) K.-X. Teng.; L.-Y. Niu.; N. Xie and Q.-Z. Yang, *Nat. Commun.,* 2022, **13**, 6179.

(8) Y. Ni.; J. Wang.; W. Ai.; Z. Yu.; X. Zhu.; S. Wang.; X. Sun.; Q. Zhang.; X. Chen.; M. Zhu and H. Zhou, *Adv. Optical Mater*., 2024, **12**, 2302834

(9) D. Xi.; M. Xiao.; J. Cao.; L. Zhao.; N. Xu.; S. Long.; J. Fan.; K. Shao.; W. Sun.; X. Yan.; X. Peng, *Adv. Mater.,* 2020, **32**, 1907855.

(10) Z. Zhang.; Q. Yuan.; M. Li.; B. Bao.; Y. Tang, *Small* 2021, **17**, 2104581.

(11) Y. Wang.; W. Zhang.; P. Sun.; Y. Cai.; W. Xu.; Q. Fan.; Q. Hu.; W. Han, *Theranostics,* 2019, **9**, 391.

(12) L. Bai.; P. Sun.; Y. Liu.; H. Zhang.; W. Hu.; W. Zhang.; Z. Liu.; Q. Fan.; L. Li.; W. Huang.; *Chem.Commun.*, 2019, **55**, 10920.

(13) Y. Xu.; S. Wang.; Z. Chen.; R. Hu.; S. Li.; Y. Zhao.; L. Liu.; J. Qu, *J. Nanobiotechnol.,* 2021, **19**, 37.

(14) C. Yao.; Y. Chen.; M. Zhao.; S. Wang.; B. Wu.; Y. Yang.; D. Yin.; P. Yu.; H. Zhang.; F. Zhang.; *Angew.Chem. Int.Ed*., 2022, **61**, e202114273.

(15) Y. Tian.; D. Yin.; Q. Cheng.; H. Dang.; C. Teng.; L. Yan, *J. Mater. Chem. B*, 2022, **10**, 1650.

(16) N. Yang.; S. Song.; C. Liu.; J. Ren.; X. Wang.; S. Zhu.; C. Yu, *Biomater. Sci.*, 2022, **10**, 4815.

(17) J. Zhang.; Y. Li.; M. Jiang.; H. Qiu.; Y. Li.; M. Gu.; S. Yin, *ACS Biomater. Sci. Eng.* 2023, **9**, 821.

(18) S. Bian.; X. Zheng.; W. Liu.; J. Li.; Z. Gao.; H. Ren.; W. Zhang.; C.-S. Lee.; P. Wang, *Biomaterials,* 2023, **298**, 122130.

(19) Z. Shi.; H. Bai.; J. Wu.; X. Miao.; J. Gao.; X. Xu.; Y. Liu.; J. Jiang.; J. Yang.; J. Zhang.; T. Shao.; B. Peng.; H. Ma.; D. Zhu.; G. Chen.; W. Hu.; L. Li.; W. Huang, *Research*, 2023, **6**, 0169.

(20) D. Chen.; Y. Xu.; Y. Wang.; C. Teng.; Xin. Li.; D. Yin.; L. Yan, *Spectrochim. Acta, Part A*, 2024, **322**, 124789.